A novel selective metabotropic glutamate receptor 4 agonist reveals new possibilities for developing subtype selective ligands with therapeutic potential

Cyril Goudet,[*,†,1] Bruno Vilar,[*,†] Tiphanie Courtiol,[‡] Thierry Deltheil,[§] Thomas Bessiron,[‖] Isabelle Brabet,[*,†] Nadia Oueslati,[*,†] Delphine Rigault,[‡] Hugues-Olivier Bertrand,[¶] Heather McLean,[‖] Hervé Daniel,[‖] Marianne Amalric,[§] Francine Acher,[‡,1] and Jean-Philippe Pin[*,†]

[*]Institut de Génomique Fonctionnelle, Centre National Recherche Scientifique (CNRS) UMR5203, Université de Montpellier, Montpellier, France; [†]Institut National de la Santé et de la Recherche Médicale, U661, Montpellier, France; [‡]Laboratoire de Chimie et Biochimie Pharmacologiques et Toxicologiques, CNRS UMR8601, Université Paris Descartes, Sorbonne Paris Cité, Paris, France; [§]Laboratoire de Neurobiologie de la Cognition, CNRS UMR6155, Aix-Marseille Université, Marseille, France; [‖]Laboratoire de Pharmacologie et Biochimie de la Synapse, CNRS UMR8619, Institut de Biochimie et de Biophysique Moléculaire et Cellulaire, Université Paris-Sud 11, Orsay, France; and [¶]Accelrys SARL, Parc-Club Université, Orsay, France

ABSTRACT **Metabotropic glutamate (mGlu) receptors are promising targets to treat numerous brain disorders. So far, allosteric modulators are the only subtype selective ligands, but pure agonists still have strong therapeutic potential. Here, we aimed at investigating the possibility of developing subtype-selective agonists by extending the glutamate-like structure to hit a nonconsensus binding area. We report the properties of the first mGlu4-selective orthosteric agonist, derived from a virtual screening hit, LSP4-2022 using cell-based assays with recombinant mGlu receptors [EC_{50}: 0.11±0.02, 11.6±1.9, 29.2±4.2 μM (n>19) in calcium assays on mGlu4, mGlu7, and mGlu8 receptors, respectively, with no activity at the group I and -II mGlu receptors at 100 μM]. LSP4-2022 inhibits neurotransmission in cerebellar slices from wild-type but not mGlu4 receptor-knockout mice. *In vivo*, it possesses antiparkinsonian properties after central or systemic administration in a haloperidol-induced catalepsy test, revealing its ability to cross the blood-brain barrier. Site-directed mutagenesis and molecular modeling was used to identify the LSP4-2022 binding site, revealing interaction with both the glutamate binding site and a variable pocket responsible for selectivity. These data reveal new approaches for developing selective, hydrophilic, and brain-penetrant mGlu receptor agonists, offering new possibilities to design original bioactive compounds with therapeutic potential.—Goudet, C., Vilar, B., Courtiol, T., Deltheil, T., Bessiron, T., Brabet, I., Oueslati, N., Rigault, D., Bertrand, H.-O., McLean, H., Daniel, H., Amalric, M., Acher, F., Pin, J.-P. A novel selective metabotropic glutamate receptor 4 agonist reveals new possibilities for developing subtype-selective ligands with therapeutic potential. *FASEB J.* 26, 1682–1693 (2012). www.fasebj.org**

Key Words: mGluR · drug development · Parkinson's disease

A GREAT CHALLENGE in pharmaceutical research is the development of selective drugs that are designed to reduce a certain side effect profile. G-protein-coupled receptors (GPCRs) are a valuable class of target in therapeutic drug development (1). However, because of the multiplicity of receptors targeted by a given transmitter or hormone and a high degree of conservation in the endogenous ligand binding site, it is generally difficult to develop receptor subtype-selective orthosteric ligands. When based on the structure of the endogenous ligand, rational drug design often produces potent, but not subtype-selective, ligands.

Abbreviations: 7TM, 7-transmembrane; ANPR, atrial natriuretic peptide receptor; CNS, central nervous system; DCPG, dicarboxyphenylglycine; EPSC, excitatory postsynaptic current; GPCR, G-protein-coupled receptor; mGlu, metabotropic glutamate; mGlu4-KO, metabotropic glutamate receptor 4 receptor knockout; PAM, positive allosteric modulator; PC, Purkinje cell; PCEP, 3-amino-3-carboxypropyl-2′-carboxyethyl phosphinic acid; PF, parallel fiber; PPF, paired-pulse facilitation, PTX, pertussis toxin, VFT, Venus flytrap; WT, wild-type.

[1] Correspondence: C.G., Institut de Génomique Fonctionnelle, CNRS UMR5203, INSERM U661, Universités de Montpellier, 141, Rue de la Cardonille, F34094 Montpellier cedex 5, France. E-mail: cyril.goudet@igf.cnrs.fr; F.A., Laboratoire de Chimie et de Biochimie Pharmacologiques et Toxicologiques, CNRS UMR8601, Université Paris Descartes, Sorbonne Paris Cité, 45, Rue des Saints-Pères, F75270 Paris cedex 6, France. E-mail: francine.acher@parisdescartes.fr

doi: 10.1096/fj.11-195941

This article includes supplemental data. Please visit *http://www.fasebj.org* to obtain this information.

0892-6638/12/0026-1682 © FASEB

This is well illustrated within metabotropic glutamate (mGlu) receptors, which play key roles in the modulation of many synapses and are considered promising targets for the treatment of various central nervous system (CNS) diseases (2–4). Eight mGlu receptors have been characterized and classified into 3 groups on the basis of their sequence similarity and functional properties. These receptors are constituted of 3 juxtaposed domains: a large bilobate extracellular domain, also called the Venus flytrap (VFT) domain, which contains the glutamate binding site; a core 7-transmembrane (7TM) domain composed of 7 helices, which is common to all GPCRs and responsible for G-protein coupling; and a cysteine-rich domain that links the VFT and 7TM domains (3). Despite major efforts to develop subtype-selective ligands for these receptors, orthosteric ligands only display group selectivity, and none can be considered as subtype selective. This is well supported by the crystal structures of the ligand binding domains of 4 of the 8 receptor subtypes (5–7), which illustrate the high degree of conservation of the glutamate-binding site among receptors from the same group (8–10).

Accordingly, high-throughput screening strategies have been conducted and led to the identification of highly selective ligands acting either as positive, negative, or neutral allosteric modulators (11). These compounds were demonstrated to bind to a site that is distinct to that of the orthosteric (glutamate-binding) site located in the VFT domain, but rather to specific sites in the 7TM domain of these receptors (3). In addition to their subtype selectivity, these compounds are very promising leads for many other reasons: their polycyclic structure offers multiple possibilities for drug design; their hydrophobicity allows them to easily cross the blood brain barrier. More important, positive allosteric modulators (PAMs), through the specific potentiation of the effect of glutamate, allow the maintenance of the spatiotemporal activity of these receptors, thereby limiting side effects and desensitization of the receptors (11).

However, limitations were identified for the development of mGlu allosteric compounds. Their hydrophobicity can limit their solubility and their bioavailability and may increase their probability of off-target actions. Although many are subtype selective, several display opposite effects on different mGlu receptor subtypes (12, 13). Furthermore, many PAMs display agonist activity (14, 15), such that mGlu PAMs become only as useful as classical agonists. Finally, although desensitization was viewed as a problem for agonist development, several mGlu receptor subtypes were found not to desensitize (16–17).

Orthosteric mGlu agonists have proven therapeutic potential, as illustrated by clinical studies (18), and in contrast to what was first anticipated, many can cross the blood-brain barrier (18–20), and their bioavailability can be improved through the synthesis of prodrugs (3, 18). Thus, we aimed to reanalyze whether specific strategies could be identified to develop subtype-selective mGlu receptor agonists.

Our goal was to examine whether extended ligands that contact both the highly conserved glutamate binding site and a less conserved area, could display better subtype selectivity. We recently employed a virtual screening strategy to identify such elongated agonists for the mGlu4 receptor subtype (21). This approach allowed us to identify new series of agonists for group III mGlu receptors (mGlu4, 6, 7 and 8 receptors; refs. 20, 22). Here, we report the characterization of LSP4-2022, a compound being >100 times more potent at the mGlu4 receptor compared to other brain mGlu receptors. We identified an additional interacting region, which we believe is responsible for the selectivity; and also demonstrated that the compound is active on the native receptor, not only in brain slices, but also *in vivo*, as further illustrated through its antiparkinsonian effects.

Taken together, our study reveals a specific region within the VFT cleft of mGlu receptors that can be targeted to develop subtype-selective ligands, thus opening new avenues for the development of novel therapeutic compounds to treat various CNS disorders. It is an additional illustration of a principle that can be of interest to develop selective drugs for other receptors.

MATERIALS AND METHODS

Cell transfection and second messenger determination

HEK293 cells were transiently transfected with mGlu receptors by electroporation, as described elsewhere (23). Group III mGlu receptors were cotransfected with a chimeric G_q/G_i protein, allowing the monitoring of receptor activity by measurements of $[Ca]_i$; and EAAC1, a glutamate transporter, to avoid the influence of extracellular glutamate. After 24 h, cells were loaded with Ca-sensitive fluorescent dye Fluo-4-AM (Invitrogen, Cergy Pontoise, France), and $[Ca]_i$ determinations were performed, as described previously (24). All points are realized in triplicate. Data were analyzed using the Prism software (GraphPad, La Jolla, CA, USA).

Site-directed mutagenesis

Mutant receptors were obtained using the Quick-Change strategy (Stratagene, La Jolla, CA, USA). All mutations were verified by sequencing. All receptors possessed an HA epitope at their N termini, allowing the determination of their cell surface expression by ELISA, as described previously (24). The mutants described in this study displayed an expression level comparable to the wild-type (WT; Supplemental Fig. S1).

Molecular modeling: docking of LSP4-2022 in mGlu4 extracellular domain

All calculations were performed in Discovery Studio 2.5.5 (Accelrys Software, San Diego, CA, USA). LSP4-2022 was docked in a previously validated homology model of the mGlu4 receptor VFT (22, 25). The ligand was initially positioned in the binding site using CDocker (26). Protein-ligand

interactions were further optimized by 1-ns molecular dynamics using CHARMM (27). Once the trajectory was equilibrated, snapshots of the trajectory were analyzed in terms of protein-ligand contacts, and those selected were submitted to energy minimization, thereby leading to the model presented in this article.

Electrophysiology on tsA-201 cells

Transfection of tsA-201 cells was performed using Lipofectamine 2000 (Invitrogen) with Cav2.2 α_1, β_{1b}, $\alpha_2\delta_1$ subunits, mGlu receptor, and CD8. Electrophysiological recordings were performed 2–3 d later on positively transfected cells identified with anti-CD8 antibody-coated beads. Whole-cell patch-clamp experiments were performed using an Axopatch 200B amplifier (Molecular Devices, Sunnyvale, CA, USA). Except where indicated in the text, currents were evoked with 400-ms depolarizing pulses from −80 mV to the potential, giving the maximum inward current delivered at 0.1 Hz. For pertussis toxin (PTX) experiments, cells were incubated overnight with 500 ng/ml before recording. Extracellular solution contained (in mM): 2 $CaCl_2$, 20 tetraethylammonium chloride, 10 HEPES, 135 NaCl, and 1 $MgCl_2$ (pH 7.3 with tetraethylammonium hydroxide). Pipettes (borosilicate glass, 2–3 MΩ) were filled with an internal solution containing (mM): 130 CsCl, 1 $MgCl_2$, 10 EGTA, 2 $CaCl_2$ 10 HEPES, 4 Mg-ATP, and 0.3 Tris-GTP (pH 7.3 with NaOH). Drug dilutions were applied to cells by gravity-driven perfusion. Recordings were filtered at 2–5 kHz. Data were analyzed using pClamp10 (Molecular Devices) and Prism software.

LSP4-2022 activity in cerebellar slices

Animal care and all experimental procedures performed adhere to government guidelines.

Mice were stunned and then decapitated. Coronal and sagittal cerebellar slices (250 mm thick) were prepared from the vermis of 25- to 51-d-old mGlu4 receptor-knockout (mGlu4-KO) and WT mice. Slices were prepared in an ice-cold (3°C) sucrose-based solution saturated with 95% O2–5% CO_2, containing (mM): 230 sucrose, 2.5 KCl, 1.25 KH_2PO_4, 8 $MgCl_2$, 25 glucose, 26 $NaHCO_3$, 0.8 $CaCl_2$ (osmolarity 330 mosmol/L) and kept at room temperature for ≥1 h before recording in saline solution gassed with 95% O_2-5% CO_2. This solution contained (in mM): 124 NaCl, 3 KCl, 24 $NaHCO_3$, 1.15 KH_2PO_4, 1.15 $MgSO_4$, 2 $CaCl_2$, and 10 glucose (osmolarity 330 mosmol/L and pH 7.35) at 25°C. The recording chamber was perfused at a rate of 2 ml/min with the oxygenated saline solution, supplemented with the $GABA_A$ receptor antagonist bicuculline methiodide (10 μM, Sigma Aldrich, St Quentin Fallavier, France).

Whole-cell patch-clamp recordings of Purkinje cells (PCs) were performed in sagittal slices with an Axopatch-1D amplifier (Molecular Devices) at 28–30°C. Patch pipettes (3.5–5 MΩ, borosilicate glass) were filled with an internal solution containing (in mM): 140 KGlu, 6 KCl, 10 HEPES, 0.75 EGTA, 1 $MgCl_2$, 0.4 Na-GTP, and 4 Na_2-ATP (pH 7.3 with KOH; 300 milliosmol/L). PCs were clamped at −70 mV, and parallel fibers (PFs) were stimulated once every 6 s, through a glass saline-filled monopolar electrode placed at the surface of the slice, in the lower half of the molecular layer, to evoke PF-mediated excitatory postsynaptic currents (EPSCs). PF-EPSCs were evoked with pairs of stimuli of the same intensity applied to the cell with an interval of 40 ms. Paired-pulse facilitation (PPF; ref. 28) was calculated online as the ratio of the amplitude of the second PF–EPSC over the first one. Mean PPF values were obtained by averaging PPFs in individual traces for each cell. In the cells conserved for analysis, access resistance (usually 5–10 MΩ) was partially compensated (50–70%), according to the procedure described by Llano *et al.* (29). Throughout the experiment, PF-mediated EPSCs were elicited on a 10-mV hyperpolarizing voltage step, which allowed monitoring of passive membrane properties. PF-mediated responses were analyzed online and offline with Acquis1 software (Biologic, Claix, France).

PF tracts were loaded with Fluo-4FF-AM (Molecular Probes, Eugene, OR, USA), and fluorescent signals were recorded with a photometer, as described previously (16, 30). Statistical significance was assessed with an unpaired Student's t test, with values of $P < 0.05$ (2-tailed) considered significant. All data are expressed as means ± SE.

LSP4-2022 activity in the haloperidol-induced catalepsy test

Handling of animals and all procedures were conducted in strict accordance with a protocol approved by the European Communities council directive (86/609/EEC, November 24th, 1986).

A first group of male Wistar rats (n=22, 300–350 g; Charles River, Oncins, France) was anesthetized with xylazine (15 mg/kg) and ketamine (100 mg/kg) and placed in a stereotactic instrument. Rats were implanted with bilateral stainless-steel guide cannulas positioned 1 mm above the left or right ventricle (coordinates: AP −0.9 mm, L ±1.8 mm, and DV −2.2 mm from bregma, incisor bar −3.0 mm). Guide cannulas were anchored to the skull, and stainless-steel wire inlet cannulas were placed inside to prevent occlusion and infection. After a 7-d recovery period, intracerebroventricular (i.c.v.) injections were performed with stainless-steel injector needles inserted inside the implanted guide cannulas and fitted so that they protruded 1 mm below, within the ventricle. Injections were carried out by gravity. The animals were tested in the catalepsy test immediately afterward. Parkinsonian motor symptoms were evaluated in the neuroleptic-induced catalepsy test. Intraperitoneal (i.p.) injection of haloperidol (1 mg/kg) produces a typical cataleptic behavior reminiscent of the parkinsonian akinesia that can be measured in the bar test. At 60 minutes after haloperidol injection, the animals received an intracerebroventricular administration of 2 μl of LSP4-2022 solution at 2 concentrations (0.005 and 0.05 nM) and were tested in the horizontal bar test immediately afterward every 30 min for the 90-min testing period. Each animal was gently placed with its forepaws on a rod, and the time that elapsed before it stepped down from the bar was recorded in seconds (with a cutoff time of 120 s). One week later, LSP4-2022 was injected intracerebroventricularly in the same animals with no prior haloperidol injection to test for potential sedative effects of LSP4-2022 by itself. Finally, a second group of rats (n=37), was administered with various doses of LSP4-2022 (0, 0.75, 1, 2, 10, and 30 mg/kg i.p.; n=7, 7, 7, 8, 4, and 4, respectively) 30 min after haloperidol to assess its effect on catalepsy after peripheral injection. Catalepsy data were analyzed by using a multiple Kruskal-Wallis H test. The median latency was calculated for each dose and for each 30-min period. Individual comparisons were performed using the nonparametric Mann-Whitney U test.

Compounds

L-AP4 was purchased from Ascent Scientific (Weston-Super-Mare, UK). Haloperidol was purchased from Sigma-Aldrich. LSP4-2022 was synthesized in the laboratory of F.A., following a procedure analogous to that previously described (22).

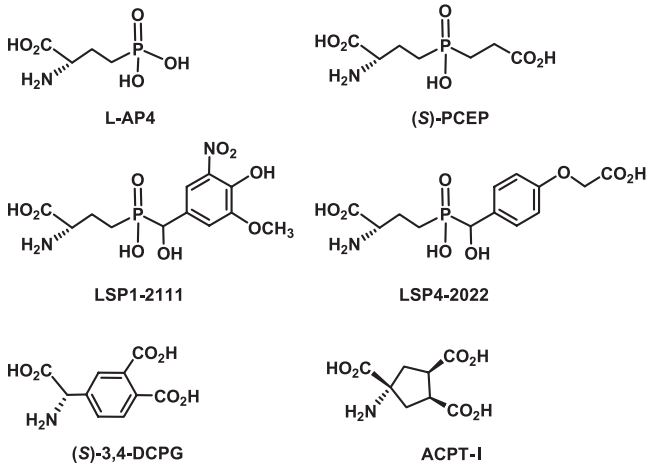

Figure 1. Structure of LSP4-2022 and other agonists of group III mGlu receptors: L-AP4, (*S*)-PCEP, ACPT-I, (*S*)-3,4-DCPG, and LSP1-2111.

RESULTS

LSP4-2022 is a selective and potent mGlu4 agonist

LSP4-2022 derives from a hit compound [3-amino-3-carboxypropyl-2′-carboxyethyl phosphinic acid (PCEP); **Fig. 1**] that was identified following a virtual screening approach aiming to examine whether extended agonists, possibly interacting with less conserved area in the vicinity of the glutamate binding site, could be identified (21). This new group III agonist is among the most potent mGlu4 agonist, with a potency of 110 ± 20 nM (n=34), similar to that of L-AP4 in HEK293 cells expressing the mGlu4 receptor (**Fig. 2** and **Table 1**). Interestingly, this agonist is displaying mGlu4 selectivity, being 256-fold, 105-fold, and 40-fold less potent at mGlu8, mGlu7, and mGlu6, respectively (Table 1). In comparison, (*S*)-3,4-dicarboxyphenylglycine (DCPG) is highly preferential for mGlu8, being 73-fold less potent on mGlu4 receptors (Fig. 2). LSP4-2022 was without effect on group I or -II mGlu receptors when tested at 100 μM. In these experiments, cell surface expression of the different receptors determined by ELISA are comparable, then ruling out that the difference in potencies could result from a difference in receptor reserve. Also it should be noted that the L-AP4 potencies measured in these cells are quite similar to potencies or affinities reported in the literature on all four group III mGlu receptors (Supplemental Fig. S1 and Table S1).

Since the agonist potency and efficacy of GPCRs can be dependent on the signaling pathway (31), we then verified that similar data could be reproduced when analyzing an endogenous signaling pathway for group III mGlu receptors. As illustrated in **Fig. 3**, LSP4-2022 dose-dependently inhibits calcium currents in tsA-201 cells expressing any group III mGlu receptors and the Cav2.2 α_{1B}, β_{1B}, and $\alpha_2\delta_1$ subunits, measured by whole-cell patch clamp. Control experiments confirmed that the observed inhibition is G protein mediated, as illustrated by the PTX sensitivity (Fig. 3*B*), and the prepulse inhibition of the effect (Fig. 3*C*).

Through the use of the natural G-protein-coupling axis of group III mGlu receptors, LSP4-2022 potencies were found comparable to those obtained with the Ca^{2+} assay (Fig. 3*D* and Table 1). Taken together, these results confirmed the potency and selectivity of LSP4-2022 on mGlu4 *vs.* the other mGlu receptors, especially when compared to the group III receptors expressed in the brain (mGlu7 and mGlu8 since mGlu6 is expressed solely in the retina).

Docking of LSP4-2022 at the mGlu4 binding site

The improved mGlu4 selectivity of LSP4-2022 compared to any other group III agonists suggests that the extended moiety of this compound targets a specific area within the VFT cleft that is less conserved than the glutamate binding site. We docked LSP4-2022 similarly to (*S*)-PCEP, the initial virtual screening hit, in a homology model of mGlu4 VFT (**Fig. 4*A–D***). These docking experiments suggested that the L-AP4-like moiety binds to the glutamate binding site and that the distal part fits to a new pocket located in lobe1 of the VFT (22). This new pocket is lined with 2 short loops: loop β2-α2 (between β-strand 2 and α-helix 2, residues 107–112) and loop β3-α3 (residues 156–159). While loop β2-α2 is conserved among all group III mGlu receptors, loop β3-α3, which is also part of the glutamate pocket, varies among these subtypes (Fig. 4*E*). We also noted that this pocket is analogous to the

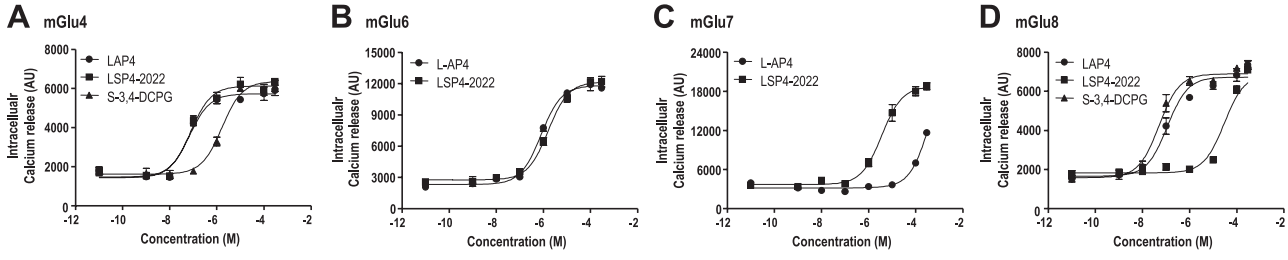

Figure 2. Concentration-response curves of LSP4-2022 on group III mGlu receptors as determined by intracellular Ca^{2+} release measurement. HEK293 cells were transiently transfected with group III mGlu receptors (mGlu4, *A*; mGlu6, *B*; mGlu7, *C*; or mGlu8, *D*) and a chimeric G protein. Receptor activation following stimulation by different concentrations of agonist was determined by intracellular Ca^{2+} release, measured using the fluorescent probe Fluo4-AM. Data points correspond to means ± SE of ≥3 experiments performed in triplicate.

TABLE 1. *Potency of L-AP4 and LSP4-2022 on WT group-III mGlu receptors and mutants of mGlu4 and mGlu8 receptors*

Receptor	L-AP4 [EC_{50} (n)]	LSP4–2022 [EC_{50} (n)]
Inhibition of CaV2.2		
mGlu4	0.08 ± 0.03 (5)	0.12 ± 0.03 (5)
mGlu6	3.15 ± 0.51 (5)	3.68 ± 0.94 (5)
mGlu7	356 ± 88 (5)	15.7 ± 3.5 (5)
mGlu8	0.16 ± 0.04 (5)	51.6 ± 10.6 (5)
Ca-assay		
mGlu4	0.13 ± 0.02 (34)	0.11 ± 0.02 (30)
mGlu6	1.03 ± 0.27 (7)	4.4 ± 0.6 (14)
mGlu7	>100 (5)	11.6 ± 1.9 (19)
mGlu8	0.29 ± 0.07 (31)	29.2 ± 4.2 (27)
mGlu4 S159A	1.97 ± 0.83 (3)	3.13 ± 1.06 (3)
mGlu4 T182A	>100	>100
mGlu4 R78A	>100 (3)	>100 (3)
mGlu4 K74A K317A	64.8 ± 2.1 (3)	0.33 ± 0.14 (3)
mGlu4 K405A	40.9 ± 10.5 (4)	2.41 ± 0.65 (3)
mGlu4 S157A	0.19 ± 0.05 (3)	0.06 ± 0.02 (3)
mGlu4 G158A	0.07 ± 0.02 (3)	3.33 ± 0.89 (3)
mGlu4 S157A G158A	0.26 ± 0.06 (11)	3.83 ± 0.83 (8)
mGlu4 Loop8	0.31 ± 0.14 (7)	0.33 ± 0.06 (5)
mGlu4 Loop8 S157A G158A	0.70 ± 0.29 (5)	49.28 ± 5.22 (5)
mGlu4 G59A S157A G158A	0.55 ± 0.09 (8)	14.97 ± 4.58 (7)
mGlu4 R60K S157A G158A	0.10 ± 0.04 (7)	3.56 ± 0.95 (6)
mGlu4 S62E S157A G158A	0.34 ± 0.10 (7)	5.67 ± 2.54 (5)
mGlu4 E63R S157A G158A	0.53 ± 0.13 (9)	6.47 ± 1.47 (10)
mGlu4 K65V S157A G158A	0.28 ± 0.12 (5)	2.65 ± 1.45 (4)
mGlu4 A66P S157A G158A	0.54 ± 0.24 (5)	4.70 ± 1.98 (5)
mGlu4 G59A E63R S157A G158A	0.70 ± 0.20 (4)	15.02 ± 6.91 (4)
mGlu8 A154S A155G	0.11 ± 0.04 (7)	0.63 ± 0.25 (6)
mGlu8 Loop4	0.11 ± 0.03 (6)	7.77 ± 4.35 (4)
mGlu8 Loop4 A154S A155G	0.09 ± 0.01 (4)	0.10 ± 0.01 (4)
mGlu4 T108A	70.9 ± 32.8 (3)	11.7 ± 3.5 (4)
mGlu4 C109A	1.13 ± 0.25 (3)	0.17 ± 0.05 (3)
mGlu4 S110A	0.14 ± 0.03 (3)	0.24 ± 0.02 (3)

For WT receptors, EC_{50} values of L-AP4 and LSP4–2022 have been determined in transfected cells by two different functional assays: ligand-induced intracellular calcium release measurement *via* the fluorescent probe, Fluo4-AM, and ligand-induced inhibition of evoked current through N-type voltage-dependent calcium channel using the whole-cell patch-clamp technique. For mutant receptors, EC_{50} values have been determined using the first functional output. EC_{50} values are expressed as means ± SE (μM) of n experiments (n given in parentheses).

chloride binding pocket in the atrial natriuretic peptide receptors (ANPRs) that possess a homologous VFT domain (refs. 22, 32 and Supplemental Fig. S2).

The glutamate-like part of LSP4-2022 binds into the orthosteric pocket of mGlu4

Residues interacting with L-AP4 and glutamate divide into those of a conserved motif binding the amino acid moiety and those of a basic cluster binding the side-chain acidic group (carboxylic or phosphonic). The proximal motif is composed of S159, A180, T182, Y230, and D312, while the basic cluster is composed of K74, R78, K317, and K405 (22, 33). Docking experiments are consistent with these residues interacting in an analogous way with LSP4-2022, except for K74 and K317, which interact with the hydroxybenzylic moiety (Fig. 4*B*). Interestingly, the 7 residues (proximal motif, R78 and K405) that bind glutamate in all mGlu receptors bind the glutamate-like part of LSP4-2022 (5–7, 10).

Mutagenesis experiments validated the proposed binding mode of LSP4-2022. Cell surface expression of mutant receptors determined by ELISA was comparable to that of WT (Supplemental Fig. S1). As expected, the S159A or T182A mutants display drastically decreased LSP4-2022 and L-AP4 potencies (Table 1), consistent with the α-amino acid moiety of both compounds interacting in a similar way in the mGlu4 receptor.

The cluster of basic residues (Fig. 4*B*) is involved in LSP4-2022 binding, but the lysine residues are less critical than for the binding of L-AP4, suggesting that other residues stabilize LSP4-2022, probably by interacting with its distal part (Table 1).

The distal moiety of LSP4-2022 binds into a pocket delineated by loop β2-α2 and loop β3-α3

Molecular docking suggested that the phenoxyacetic acid group of LSP4-2022 interacts in a cavity within the lobe-I of mGlu4 VFT, delineated by 2 short loops (β2-α2 and

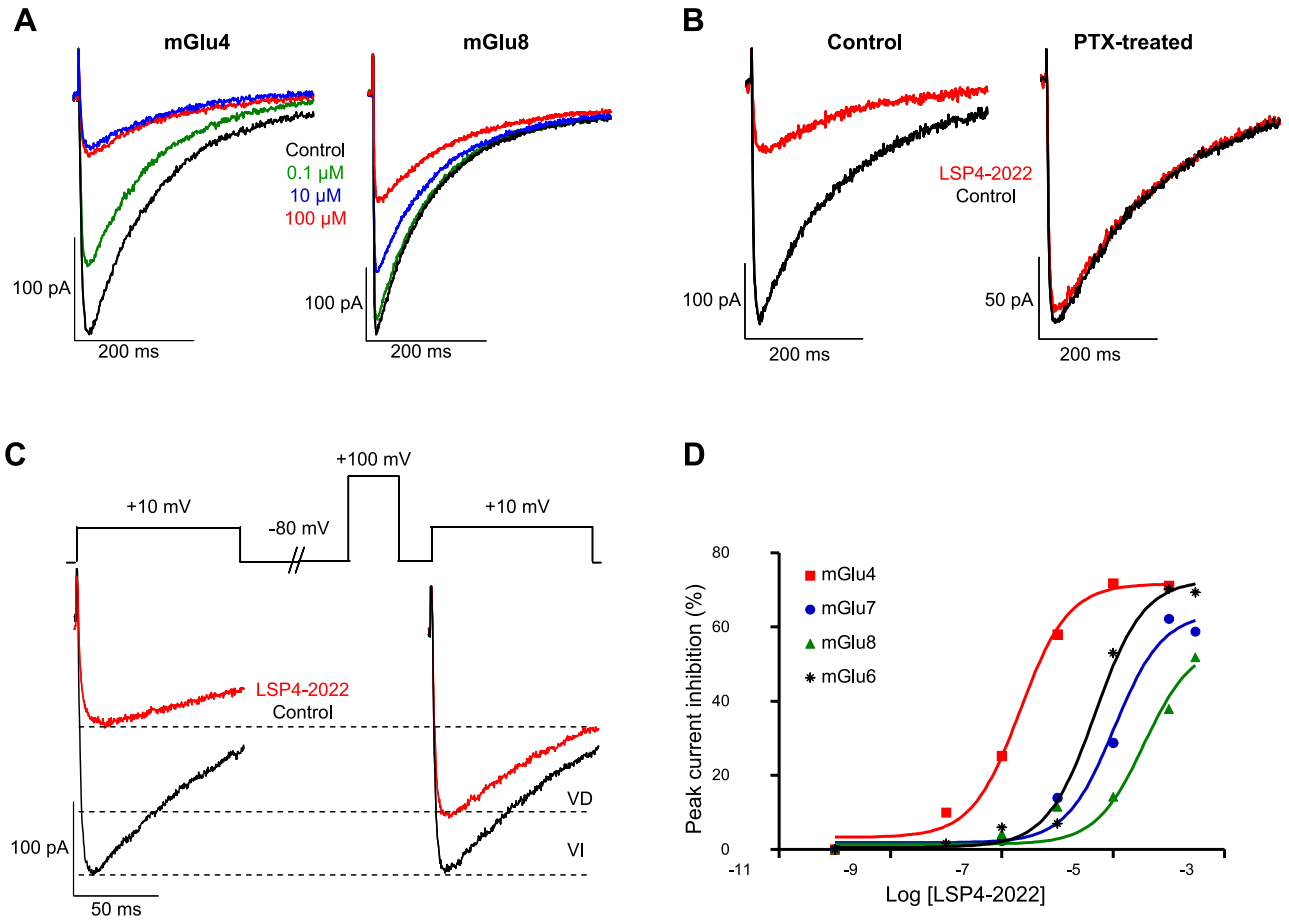

Figure 3. Inhibition of N-type voltage-gated calcium channel induced by activation of group III mGlu receptors by LSP4-2022. Ca^{2+} currents were recorded by whole-cell patch clamp in tsA-201 cells transiently transfected with N-type calcium channels (Cav2.2 α1, β2 and α1δ) and group III mGlu receptors (mGlu4, mGlu6, mGlu7, or mGlu8). *A*) Superimposed traces of peak Ca^{2+} current through N-type calcium channels in absence and presence of different concentrations of LSP4-2022, recorded at +10 mV in mGlu4 or mGlu8 receptor-expressing cells. *B*) Blockade of LSP4-2022-induced inhibition of Ca^{2+} currents following the pretreatment with PTX in mGlu4-expressing cells. *C*) Decrease of LSP4-2022-induced inhibition of Ca_{2+} currents following a depolarizing prepulse at +100 mV before the test pulse, in cells expressing mGlu4 receptor. VD, voltage-dependent fraction of current; VI, voltage-independent fraction of current. *D*) Dose-dependent inhibition of peak Ca^{2+} by LSP4-2022 in cells expressing N-type calcium channel and the different group III mGlu receptors. Data are representative of ≥3 experiments.

β3-α3; Fig. 4*A*, *E*). S157, G158, and T108 make hydrogen bonds with the carboxylate, while the protons of G158 (1 α-proton) and S157 (1 methylene proton) are in close contact with the phenyl ring (Fig. 4*C*). When the G158 proton is replaced by a methyl group, as in A155 of mGlu8, a steric clash is observed with the phenoxy-acetic component of LSP4-2022 (Fig. 4*D* and Table 1) if the other residues of the pocket are not forced away. This situation may explain why LSP4-2022 cannot bind with high affinity to mGlu8 and is thus mGlu4 selective.

Mutations in the β2-α2 loop revealed that T108 is important for both L-AP4 and LSP4-2022 potency, while mutation of Ser110 had almost no effect (Table 1). S157 and G158 in mGlu4 β3-α3 loop are replaced by two alanines in the mGlu8 receptor and may be responsible for mGlu4/8 selectivity, as suggested by molecular models (Fig. 4*D* and Table 1). Changing G158 of mGlu4 receptor with A155, as found in mGlu8 receptor, had no effect on L-AP4 potency, but significantly decreased LSP4-2022 potency, though it did not reach that measured at mGlu8. Conversely, in mGlu8, mutation of this residue into its mGlu4 counterpart increased LSP4-2022 potency but is not sufficient to fully recover a mGlu4-like potency (Table 1 and **Fig. 5*A*, *B***). Mutations S157A in mGlu4 and A154S in mGlu8 had almost no effect, demonstrating that while the hydrophobic contacts are similar in both mutants, the hydrogen binding of the hydroxymethylene of Ser in mGlu4 does not provide additional stabilization to the backbone NH (Supplemental Fig. S3). On the other hand, our data indicate that G158 is involved in the structural network that defines LSP4-2022 binding, and therefore, its selectivity, but that other residues are also involved.

Molecular determinants of LSP4-2022 selectivity for mGlu4

Loop β1-α1 that varies in the different mGlu receptors may possibly control the size of the cavity identified

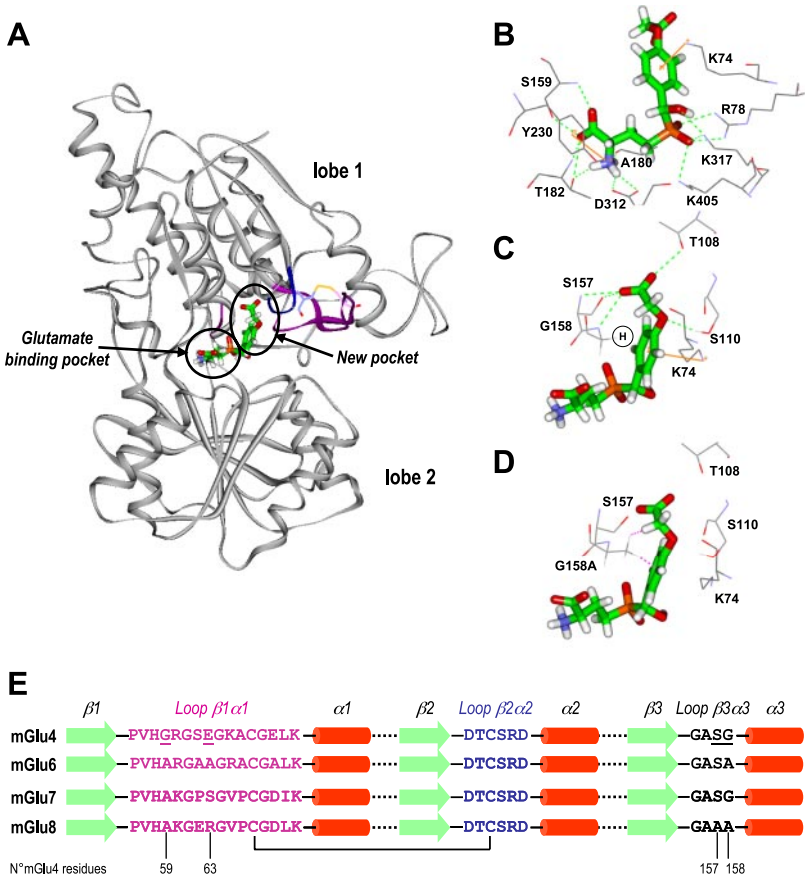

Figure 4. Docking of LSP4-2022 in the mGlu4 receptor VFT domain. *A*) Two distinct LSP4-2022 binding pockets. The glutamate pocket is found between the two lobes close to the hinge of the VFT domain; the new pocket is a small region in lobe 1, adjacent to the glutamate pocket and delimited by two short loops (loop β2-α2 and β3-α3). *B*) Expanded view of the LSP4-2022 docking, showing the conserved motif of residues binding the α-amino acid moiety and the distal cluster of basic residues. *C*) Identical orientation, except the residues binding the phenoxyacetic moiety of LSP4-2022 are shown. S157 and G158 are part of loop β3-α3, T108, and S110 of loop β2-α2. Hydrogen atom of G158 that is replaced by a methyl group in mGlu8 receptor is circled. *D*) Molecular model with G158 mutated to alanine, showing steric hindrance (magenta dashed lines) with LSP4-2022. Color code: protein ribbon, gray; loop β1-α1, magenta; loop β2-α2, dark blue; disulfide bridge between the two loops is displayed; carbon atoms, green in LSP4-2022, gray in mGlu4 receptor; oxygen atoms, red; nitrogen atoms, blue, hydrogen atoms, white; phosphorus atoms, orange. Hydrogen bonds are depicted as green dashed lines, cation-π interactions as orange lines. *E*) Alignment of the three loops of group III mGlu receptors involved in the size of the new pocket.

above. Indeed, loops β1-α1 and β2-α2 are held together by a disulfide bridge, between C67 and C109, and a network of hydrogen bonds and ionic interactions in the mGlu4 receptor (Fig. 5*D*). In agreement with this postulate, swapping loop β1-α1 between mGlu4 and mGlu8 differentially affected LSP4-2022 potency (Fig. 5*C* and Table 1), without affecting that of L-AP4. Finally, the potency of LSP4-2022 at an mGlu4 receptor mutant carrying both the S157A-G158A mutations and the mGlu8 loop was similar to that measured on the WT mGlu8. Similarly, the reverse mutant on the mGlu8 receptor displayed an LSP4-2022 potency similar to that of the mGlu4 receptor (Table 1 and Fig. 5*A*, *B*). Point mutations within the β1-α1 loop revealed that G59 and E63 of the mGlu4 receptor are particularly important for LSP4-2022 potency (Table 1).

Taken together, these results revealed the importance of the β1-α1 loop in determining the size of the

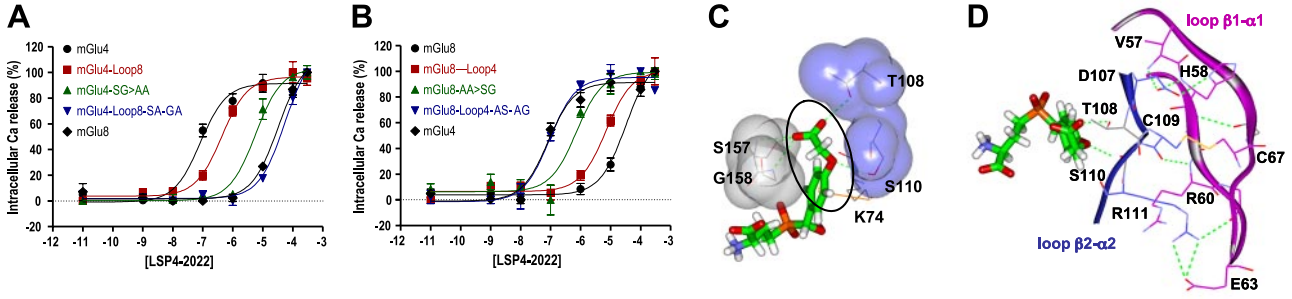

Figure 5. Molecular determinants of LSP4-2022 selectivity for mGlu4 *vs.* mGlu8 receptors. Selectivity of LSP4-2022 for mGlu4 *vs.* mGlu8 is determined by the interaction with 2 residues of the glutamate binding pocket and a loop between the first β-strand and α-helix. *A*) Concentration-response curves of LSP4-2022 on mGlu4 and mGlu8 receptors, and on mGlu4-S157A-G158A, mGlu4-loop8 (in which the loop β1-α1 of mGlu4 is replaced by the corresponding loop of mGlu8, see text for details) and mGlu4-loop8-S157A-G158A mutant receptors. *B*) Concentration-response curves of LSP4-2022 on mGlu4 and mGlu8 receptors, and on mGlu8-A154S-A155G, mGlu8-loop4 (in which the loop β1-α1 of mGlu8 is replaced by the corresponding loop of the mGlu4 receptor) and mGlu8-loop8-A154S-A155G mutant receptors. *C*) New pocket between loop β2-α2 and loop β3-α3 circled in black. *D*) Size of the new pocket is affected by loop β1-α1, tightly bound to loop β2-α2. Residues D107, C109, R111, from loop β2-α2 (dark blue) interact with V57, H58, R60, E63, from loop β1-α1 (magenta). Several of the hydrogen bonds occur with the receptor main chain, while charged side chains secure ionic interaction (*e.g.*, D107-H58, R111-E63). Atom colors as in Fig. 4.

new pocket and then the selectivity of LSP4-2022 for mGlu4 over mGlu8.

LSP4-2022 inhibits excitatory neurotransmission in cerebellar slices through mGlu4 activation

LSP4-2022 inhibits transmission at the PF-PC synapses in cerebellar slices, where the mGlu4 receptor is well known to play a crucial role. In WT PC synapses, 100 μM LSP4-2022 reversibly depressed both the first and the second PF-mediated EPSCs evoked by 2 successive stimuli, by 31.1 ± 2.1 and 24.5 ± 1.5%, respectively (n=15, **Fig. 6*A***), similar to that obtained with 100 μM L-AP4 (34). In contrast, in mGlu4-KO mice, the LSP4-2022 had no significant depressant effects (0.84±1.58 and 0.76±0.82% for first and second EPSCs, respectively; n=10; Fig. 6*D*).

LSP4-2022-induced decrease in PF-EPSCs was accompanied by a significant (P<0.05) increase in PPF, from 1.62 ± 0.04 to 1.85 ± 0.05% (Fig. 6*B*, n=15). This suggests a decrease in the probability of glutamate release (35) consistent with a presynaptic action of LSP4-2022. No such effect was observed in the mGlu4-KO mice (mean PPF: 1.49±0.05 control condition *vs.* 1.52±0.05% end of agonist application, n=10, Fig. 6*E*).

Presynaptic action of LSP4-2022 was confirmed in coronal rat cerebellar slices with fluorometric methods, using the low-affinity Ca^{2+}-sensitive dye Fluo-4FF-AM, as described previously (ref. 16 and Fig. 6*C*, inset). In WT slices, 100 μM LSP4-2022 reversibly decreased the amplitude of presynaptic Ca^{2+} transients evoked by PF stimulations by 10.7 ± 1.3%, (n=14, Fig. 6*C*), whereas no effect was observed in mGlu4-KO slices (0.6±0.9%, n=6, Fig. 6*E*).

These data indicate that LSP4-2022 is an effective agonist of native mGlu4 receptors, and further illustrate the absence of side effects of the compound, particularly on ionotropic glutamate receptors.

Antiparkinsonian action of LSP4-2022

The *in vivo* activity of LSP4-2022 was assessed on haloperidol-induced catalepsy, a classical model of parkinsonian akinesia, after either i.c.v. or systemic administration.

Haloperidol (1 mg/kg) induced a profound akinesia (*e.g.*, incapacity to step down from the bar) for the duration of the test (90 min). LSP4-2022 administered at a concentration of 0.005 mM i.c.v. significantly reduced this state at the first time point of the test (**Fig. 7*A***, P<0.05, Mann-Whitney U test). Inhibition of catalepsy was observed up to 60 min, although only being close to statistical significance at t = 30 and t = 60 min. At 0.05 mM, LSP4-2022 significantly reduced the catalepsy at the first time point (Fig. 7*A*). Overall, LSP4-2022, at the 2 doses tested, significantly counteracted haloperidol-induced catalepsy immediately after i.c.v. injection (Fig. 7*A*), and a progressive return to the cataleptic state was observed after 30 to 60 min, respectively. LSP4-2022 did not produce catalepsy when tested alone.

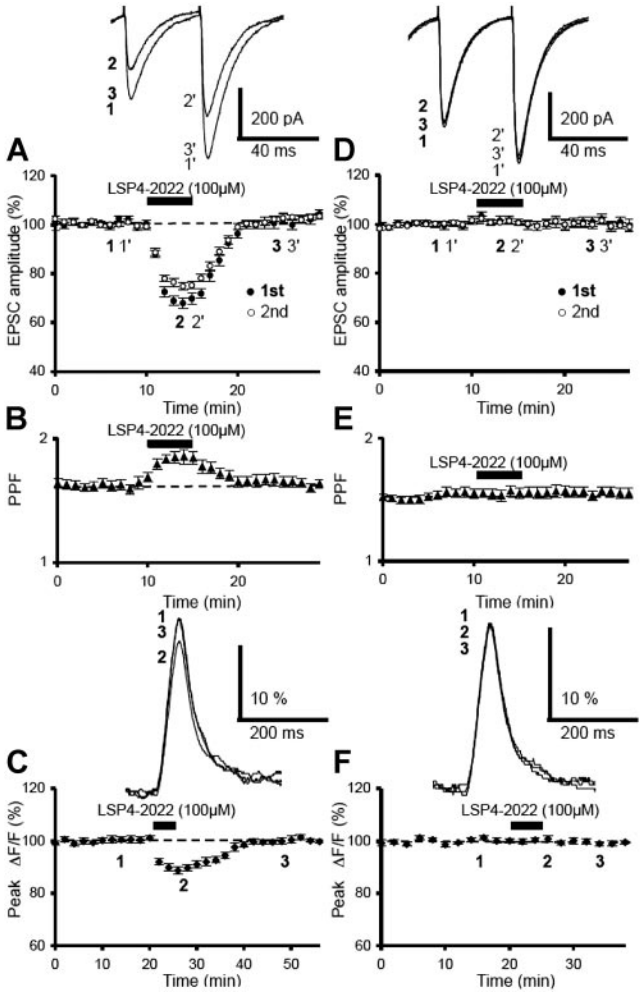

Figure 6. Inhibition of glutamatergic transmission by LSP4-2022 in cerebellar slices. Effect of LSP4-2022 on PC EPSCs and on presynaptic calcium transients evoked by PF stimulation. *A*, *D*) Time course of the normalized amplitudes of PF-mediated EPSCs before, during, and after bath application of 100 μM LSP4-2022 in WT mice (*A*) or mGlu4-KO mice (*D*). Note the lack of effect of LSP4-2022 in mGlu4-KO mice. Top insets display superimposed representative traces of PF-mediated EPSCs in PCs evoked by 2 successive stimulations with an interval of 40 ms before (*1*, *1′*), during (*2*, *2′*), and after (*3*, *3′*) agonist application. *B*, *E*) LSP4-2022-reversible depression of PF-mediated EPSCs is accompanied by a transient increase in PPF in WT (*B*) but not in mGlu4-KO mice (*E*). *C*, *F*) Time course of normalized amplitudes of peak Fluo4-FF fluorescence before, during, and after bath application of LSP4-2022 (100 μM) in WT mice (*C*) or mGlu4-KO mice (*F*). Top insets display averaged fluorescence changes, recorded at the indicated times. Fluorescence transients are reversibly depressed by LSP4-2022 bath application in WT mice but not in mGlu4-KO mice. Error bars indicate means ± SE.

To verify whether LSP4-2022 counteracts haloperidol-induced catalepsy after systemic administration, a dose-response study with LSP4-2022 was carried out in another group of rats. Doses of 0.75, 1, and 2 mg/kg of LSP4-2022 significantly reversed haloperidol-induced catalepsy at the first time point (Fig. 7*B*), and a return

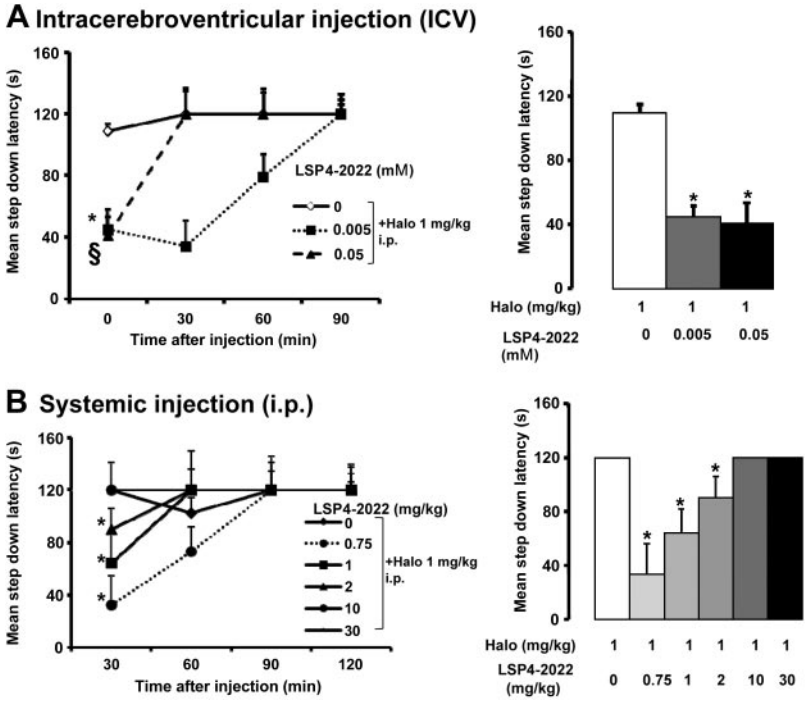

Figure 7. LSP4-2022 reverses haloperidol-induced catalepsy after either central or systemic administration. *A*) Time course effect of LSP4-2022 (0; 0.005 and 0.05 mM, n=8, 7, and 7, respectively, by dose) after i.c.v. administration on the median latency to step down from the bar and mean median latency during the first 30-min test period. *B*) Time course effect of LSP4-2022 after intraperitoneal injection (0, 0.75, 1, 2, 10, and 30 mg/kg; n=7, 7, 7, 8, 4, and 4, respectively) on the median latency to step down from the bar and mean median latency during the first 30-min test period. Halo, haloperidol. $^{*}P < 0.05$ *vs.* haloperidol, $^{\S}P < 0.05$ for 0.1 nmol *vs.* haloperidol; Mann-Whitney U test, after significant Kruskal-Wallis analysis.

to the cataleptic state was generally observed between 30 and 60 min (P<0.05 Mann-Whitney U test, after significant Kruskal-Wallis analysis). LSP4-2022 injected at the lower dose of 0.75 mg/kg produced a prolonged anticataleptic action up to 90 min. Higher doses of 10 and 30 mg/kg had no effect. These results indicate that LSP4-2022 is able to cross the blood-brain barrier to produce its antiparkinsonian effect. The optimal effect observed at low doses reveal the high potency of LSP4-2022 at mGlu4 receptors to reverse the parkinsonian symptoms.

DISCUSSION

The identification of mGlu receptor subtype-selective compounds (potency difference >100) has been hampered by the high conservation of the residues that form the glutamate binding pocket. Accordingly, no subtype-selective orthosteric ligands had been reported to date. The only subtype-selective ligands available are allosteric modulators, which bind to a site topographically distinct and less conserved among mGlu receptor subtypes. The present study reports the first selective mGlu4 orthosteric agonist, LSP4-2022. This compound illustrates a novel approach for designing subtype-selective orthosteric mGlu receptor agonists by extending the agonist molecule, allowing it to simultaneously interact to 2 distinct binding regions: the glutamate binding site and a less conserved site within the VFT cleft. This new selective mGlu4 receptor agonist is shown to be active on native receptors and to display antiparkinsonian activity, demonstrating its ability to cross the blood-brain barrier.

We have shown that LSP4-2022 is a selective mGlu4 agonist that is 100-fold more potent at this receptor subtype than at any other group III mGlu receptors expressed in the brain (but only 40-fold more potent than on the retinal mGlu6 receptor), and being inactive on any other mGlu receptors. LSP4-2022 inhibits transmission at the parallel fiber-PC synapses in cerebellar slices from WT mice, but not in those from mGlu4-KO mice, demonstrating that this compound is active in native tissues and devoid of activity on other glutamate receptors. There is a growing interest in the mGlu4 receptor as a drug target, particularly for the treatment of Parkinson's disease (4) and pain (36). Here, we show that LSP4-2022 possesses antiparkinsonian properties. Indeed, when injected in rats, this compound reversed haloperidol-induced catalepsy, a model of parkinsonian akinesia, not only following central injection but, most important, when injected systemically. This illustrates that LSP4-2022, like several other glutamate analogues (18–19), including LSP1-2111 (20), is able to cross the blood-brain barrier. LSP4-2022 has a potent anticataleptic action at a low concentration compared with LSP1-2111 when tested in the same conditions. Interestingly, the duration of this effect is reduced as the concentration increases. This may be caused by the high affinity of LSP4-2022 for mGlu7 receptors in addition to mGlu4 receptors. As previously evidenced, mGlu4 receptors are believed to underlie most of group III antiparkinsonian effects (4), while mGlu7 receptor activation in selective basal ganglia nuclei (*i.e.*, the substantia nigra reticulata) may account for adverse effects on parkinsonian symptoms (37). LSP4-2022, as well as other group III orthosteric agonists, may thus offer most promise from a therapeutic perspective because of their high solubility and effectiveness after systemic administration.

The structural originality of LSP4-2022 lies in its extended structure, which allows simultaneous binding into 2 distinct pockets of the mGlu4 VFT. This compound is composed of a glutamate-like component made of an amino acid phosphinate, which is linked to an aromatic phenoxyacetic acid moiety (Fig. 1). Docking and mutagenesis experiments confirmed that LSP4-2022 simultaneously binds into two pockets in the mGlu4 VFT, the conserved glutamate binding site is already well characterized (10, 33, 38–41), and a less conserved pocket that is largely responsible for its selectivity.

The selectivity results from selective accommodation of its phenoxyacetic moiety in the novel, less conserved pocket. While this is the case at the mGlu4 receptor subtype, the cavity is too small in the mGlu8 receptor. Two amino acids of loop β3-α3 (S157 and G158 in mGlu4) and loop β1-α1 determine the size of this distal cavity (adjacent to the glutamate site) and are thus responsible for the selectivity of LSP4-2022. S157 and G158 of mGlu4 are the only two amino acids of the glutamate binding pocket that differ between mGlu4 and mGlu8 receptors and are involved in the preferential binding of the agonist, FP429 at the mGlu4 receptor (42). Similarly, at the mGlu8 receptor with alanines at equivalent positions, the agonist, 3,4-(S)-DCPG, binds preferentially at the mGlu8 receptor compared to the mGlu4 receptor (42). The more distal loop β1-α1 indirectly affects LSP4-2022 binding; this loop is tightly bound to loop β2-α2 and holds the main differences between mGlu4 and mGlu8 receptors. At the mGlu6 and mGlu7 receptors, the same loops define the size of the distal pocket. The mGlu6 pocket varies from the mGlu4 one by an Ala in place of G157 and a Gln in place of K74. Our data show that K74 is not critical for selectivity, and the G157A mutant does show similar potency as mGlu6 (see Table 1). Thus, our mutational data allow us also to interpret the mGlu6 potency. Regarding mGlu7, the critical residues S157 and G158 of mGlu4 are conserved, allowing the binding of the oxyacetic side chain in the new pocket. The mGlu7 increased potency is thus analogous to that observed with mGlu4. However, the potency of LSP4-2022 at mGlu7 remains weaker because of the same structural feature that may explain the very low affinity/potency of most group III orthosteric agonists at mGlu7. Indeed, this specific property does not appear to be solely due to residues contacting agonists, but instead to a specific loop of the second lobe of the VFT that likely prevents a good stabilization of the active closed form of the binding domain (40). In addition, the distal part of LSP4-2022 does not fit in analogous binding pockets in group I and II mGlu receptors.

As hypothesized from the initial virtual screen, which suggested that the binding of the hit compound (*S*)-PCEP and its derivative LSP1-2093 involved a site that is analogous to the chloride binding pocket of the ANPR (22), we have now confirmed that this exosite is delimited by loops β2-α2 and β 3-α3 (32). The critical role of the homologous serine binding the chloride ion in ANPR, has been demonstrated by Ogawa *et al.* (32). This suggests that this additional pocket in the VFT cleft can serve as a binding site and may potentially be exploited to design selective ligands for other mGlu receptors.

The possibility to develop selective ligands by extending the ligand itself to reach a distinct binding pocket has already been used for other targets, such as β2-adrenergic receptors (43) or cyclooxygenases (44). However, this is the first demonstration of this strategy to develop mGlu-selective ligands acting in the VFT domain.

Interestingly, potent taste-enhancing molecules have been recently described, which bind in the VFT of sweet and umami taste receptors (two other class-C GPCRs, similar to mGlu receptors), in a pocket located close to the orthosteric binding site (45). Although this site is not homologous to the pocket that we have identified at the binding pocket of LSP4-2022; this observation suggests that it may also be possible to identify mGlu receptor PAMs that bind concomitantly with glutamate, in the VFT cleft. Such molecules can be more polar than previously identified mGlu receptor PAMs, and, like these taste enhancers, could act as pure PAMs, in contrast to those acting in the 7TM of mGlu receptors that display agonist activity in most cases. This may prove to be advantageous in order to decrease possible off-target activity and solubility issues of existing hydrophobic PAMs of mGlu receptors. If this can be verified, then LSP4-2022 could be qualified as a dual steric ligand (46), corresponding to the fusion of a nonselective orthosteric agonist with a subtype selectivity filter carried by an allosteric compound.

Much emphasis has been made regarding the advantages of positive allosteric compounds over orthosteric agonists (11), including not only their subtype selectivity, but above all their capacity to enhance receptor activity, thus allowing a maintenance of the spatiotemporal activation of the targeted receptor. However, the current mGlu4 PAMs display limited solubility, as well as robust agonist activity (15), making LSP4-2022-like compounds still interesting molecules to unravel mGlu4 receptor functional roles *in vivo*.

In summary, although selectivity of orthosteric ligands among receptor subtypes is generally difficult to achieve, the existence of the second binding pocket that we have highlighted in mGlu receptor VFT could be crucial to the development of new series of extended orthosteric ligands able to discriminate between the different mGlu receptor subtypes. Alternatively, this could be an approach for discovering new allosteric compounds that can act simultaneously with glutamate, in the VFT cleft. Such compounds may cross the blood-brain barrier, as revealed here by the central activity of LSP4-2022 following systemic injection. Overall, this new family of orthosteric agonists may be a valuable alternative to allosteric modulators for the treatment of CNS diseases. They will also provide new pharmacological tools with unprecedented properties. FJ

This work was supported by the Fondation pour la Recherche Médicale (INE20050303431), by the Agence Nationale pour la Recherche directly (ANR-05-NEUR-0121-04 and ANR-07-NEURO-047-01) or as part of the Era-net Neuron program (ANR-08-NEUR-006), by the CNRS (Direction de l'Innovation et des Relations avec les Entreprises, to T.C.), by the Ministère de l'Education Nationale, de la Recherche et de la Technologie (scholarships to T.B. and B.V.), and by the Société Française d'Etude et de Traitement de la Douleur and the Institut UPSA de la Douleur. The calcium measurements were performed using the ARPEGE (Pharmacology Screening-Interactome) platform facility at the Institute of Functional Genomics (Montpellier, France). The authors thank Emmanuel Bourinet for his help in developing the electrophysiological assay of mGlu receptor activity, Pr. Terrance P. Snutch (University of British Columbia, Vancouver, BC, Canada) for kindly providing the cDNAs of the different Cav subunits, Dr. Gregory Stewart for critical reading of the manuscript, Dr. Gérard Sadoc (Unité de Neurosciences Integratives et Computationnelles, UPR CNRS 2191, Institut Alfred Fessard, Gif-sur-Yvette, France) for providing the Acquis1 software employed in these studies, C. Vol for her involvement in the ARPEGE facility and in the J.P.P. research laboratory, and Dr. L. Prézeau for his constant support. B.V., I.B., and N.O. performed the pharmacological and mutagenesis studies under the direct supervision of C.G., who designed the study and analyzed data. T.C. and D.R. synthesized the molecules under the supervision of F.A. T.B. and H.M.L. performed the slice recordings under the supervision of H.D. T.D. performed the *in vivo* experiments under the supervision of M.A. H.O.B. was in charge of the molecular modeling, and F.A. analyzed the models. C.G. and J.P.P. wrote the manuscript, and C.G., F.A., and J.P.P. supervised the entire project.

REFERENCES

1. Overington, J. P., Al-Lazikani, B., and Hopkins, A. L. (2006) How many drug targets are there? *Nat Rev. Drug Discov.* **5,** 993–996
2. Niswender, C. M., and Conn, P. J. (2010) Metabotropic glutamate receptors: physiology, pharmacology, and disease. *Annu. Rev. Pharmacol. Toxicol.* **50,** 295–322
3. Kniazeff, J., Prezeau, L., Rondard, P., Pin, J. P., and Goudet, C. (2011) Dimers and beyond: the functional puzzles of class C GPCRs. *Pharmacol. Ther.* **130,** 9–25
4. Duty, S. (2010) Therapeutic potential of targeting group III metabotropic glutamate receptors in the treatment of Parkinson's disease. *Br. J. Pharmacol.* **161,** 271–287
5. Kunishima, N., Shimada, Y., Tsuji, Y., Sato, T., Yamamoto, M., Kumasaka, T., Nakanishi, S., Jingami, H., and Morikawa, K. (2000) Structural basis of glutamate recognition by a dimeric metabotropic glutamate receptor. *Nature* **407,** 971–977
6. Muto, T., Tsuchiya, D., Morikawa, K., and Jingami, H. (2007) Structures of the extracellular regions of the group II/III metabotropic glutamate receptors. *Proc. Natl. Acad. Sci. U. S. A.* **104,** 3759–3764
7. Tsuchiya, D., Kunishima, N., Kamiya, N., Jingami, H., and Morikawa, K. (2002) Structural views of the ligand-binding cores of a metabotropic glutamate receptor complexed with an antagonist and both glutamate and Gd^{3+}. *Proc. Natl. Acad. Sci. U. S. A.* **99,** 2660–2665
8. Parmentier, M. L., Galvez, T., Acher, F., Peyre, B., Pellicciari, R., Grau, Y., Bockaert, J., and Pin, J. P. (2000) Conservation of the ligand recognition site of metabotropic glutamate receptors during evolution. *Neuropharmacology* **39,** 1119–1131
9. Wellendorph, P., and Brauner-Osborne, H. (2009) Molecular basis for amino acid sensing by family C G-protein-coupled receptors. *Br. J. Pharmacol.* **156,** 869–884
10. Bertrand, H.-O., Bessis, A.-S., Pin, J.-P., and Acher, F. C. (2002) Common and selective molecular determinants involved in metabotropic glutamate receptor agonist activity. *J. Med. Chem.* **45,** 3171–3183
11. Conn, P. J., Christopoulos, A., and Lindsley, C. W. (2009) Allosteric modulators of GPCRs: a novel approach for the treatment of CNS disorders. *Nat. Rev. Drug Discov.* **8,** 41–54
12. Maj, M., Bruno, V., Dragic, Z., Yamamoto, R., Battaglia, G., Inderbitzin, W., Stoehr, N., Stein, T., Gasparini, F., Vranesic, I., Kuhn, R., Nicoletti, F., and Flor, P. J. (2003) (-)-PHCCC, a positive allosteric modulator of mGluR4: characterization, mechanism of action, and neuroprotection. *Neuropharmacology* **45,** 895–906
13. Mathiesen, J. M., Svendsen, N., Brauner-Osborne, H., Thomsen, C., and Ramirez, M. T. (2003) Positive allosteric modulation of the human metabotropic glutamate receptor 4 (hmGluR4) by SIB-1893 and MPEP. *Br. J. Pharmacol.* **138,** 1026–1030
14. Mitsukawa, K., Yamamoto, R., Ofner, S., Nozulak, J., Pescott, O., Lukic, S., Stoehr, N., Mombereau, C., Kuhn, R., McAllister, K. H., van der Putten, H., Cryan, J. F., and Flor, P. J. (2005) A selective metabotropic glutamate receptor 7 agonist: activation of receptor signaling via an allosteric site modulates stress parameters in vivo. *Proc. Natl. Acad. Sci. U. S. A.* **102,** 18712–18717
15. Niswender, C. M., Johnson, K. A., Weaver, C. D., Jones, C. K., Xiang, Z., Luo, Q., Rodriguez, A. L., Marlo, J. E., de Paulis, T., Thompson, A. D., Days, E. L., Nalywajko, T., Austin, C. A., Williams, M. B., Ayala, J. E., Williams, R., Lindsley, C. W., and Conn, P. J. (2008) Discovery, characterization, and antiparkinsonian effect of novel positive allosteric modulators of metabotropic glutamate receptor 4. *Mol. Pharmacol.* **74,** 1345–1358
16. Abitbol, K., Acher, F., and Daniel, H. (2008) Depression of excitatory transmission at PF-PC synapse by group III metabotropic glutamate receptors is provided exclusively by mGluR4 in the rodent cerebellar cortex. *J. Neurochem.* **105,** 2069–2079
17. Lennon, S. M., Rivero, G., Matharu, A., Howson, P. A., Jane, D. E., Roberts, P. J., and Kelly, E. (2010) Metabotropic glutamate receptor mGlu2 is resistant to homologous agonist-induced desensitization but undergoes protein kinase C-mediated heterologous desensitization. *Eur. J. Pharmacol.* **649,** 29–37
18. Patil, S. T., Zhang, L., Martenyi, F., Lowe, S. L., Jackson, K. A., Andreev, B. V., Avedisova, A. S., Bardenstein, L. M., Gurovich, I. Y., Morozova, M. A., Mosolov, S. N., Neznanov, N. G., Reznik, A. M., Smulevich, A. B., Tochilov, V. A., Johnson, B. G., Monn, J. A., and Schoepp, D. D. (2007) Activation of mGlu2/3 receptors as a new approach to treat schizophrenia: a randomized Phase 2 clinical trial. *Nat. Med.* **13,** 1102–1107
19. Palucha-Poniewiera, A., Novak, K., and Pilc, A. (2009) Group III mGlu receptor agonist, ACPT-I, attenuates morphine-withdrawal symptoms after peripheral administration in mice. *Prog. Neuropsychopharmacol. Biol. Psychiatry* **33,** 1454–1457
20. Beurrier, C., Lopez, S., Revy, D., Selvam, C., Goudet, C., Lherondel, M., Gubellini, P., Kerkerian-LeGoff, L., Acher, F., Pin, J. P., and Amalric, M. (2009) Electrophysiological and behavioral evidence that modulation of metabotropic glutamate receptor 4 with a new agonist reverses experimental parkinsonism. *FASEB J.* **23,** 3619–3628
21. Triballeau, N., Acher, F., Brabet, I., Pin, J. P., and Bertrand, H. O. (2005) Virtual screening workflow development guided by the "receiver operating characteristic" curve approach. Application to high-throughput docking on metabotropic glutamate receptor subtype 4. *J. Med. Chem.* **48,** 2534–2547
22. Selvam, C., Oueslati, N., Lemasson, I. A., Brabet, I., Rigault, D., Courtiol, T., Cesarini, S., Triballeau, N., Bertrand, H. O., Goudet, C., Pin, J. P., and Acher, F. C. (2010) A virtual screening hit reveals new possibilities for developing group III metabotropic glutamate receptor agonists. *J. Med. Chem.* **53,** 2797–2813
23. Brabet, I., Parmentier, M. L., De Colle, C., Bockaert, J., Acher, F., and Pin, J. P. (1998) Comparative effect of L-CCG-I, DCG-IV and gamma-carboxy-L-glutamate on all cloned metabotropic glutamate receptor subtypes. *Neuropharmacology* **37,** 1043–1051
24. Goudet, C., Gaven, F., Kniazeff, J., Vol, C., Liu, J., Cohen-Gonsaud, M., Acher, F., Prezeau, L., and Pin, J. P. (2004) Heptahelical domain of metabotropic glutamate receptor 5 behaves like rhodopsin-like receptors. *Proc. Natl. Acad. Sci. U. S. A.* **101,** 378–383
25. Bessis, A.-S., Bertrand, H.-O., Galvez, T., De Colle, C., Pin, J.-P., and Acher, F. (2000) Three-dimensional model of the

extracellular domain of the type 4a metabotropic glutamate receptor: new insights into the activation process. *Prot. Sci.* **9,** 2200–2209
26. Wu, G., Robertson, D. H., Brooks, C. L., 3rd, and Vieth, M. (2003) Detailed analysis of grid-based molecular docking: A case study of CDOCKER-A CHARMm-based MD docking algorithm. *J. Comput. Chem.* **24,** 1549–1562
27. Brooks, B. R., Bruccoleri, R. E., Olafson, B. D., States, D. J., Swaminathan, S., and Karplus, M. (1983) CHARMM: A program for macromolecular energy, minimization, and dynamics calculations. *J. Comp. Chem.* **4,** 187–217
28. Atluri, P. P., and Regehr, W. G. (1996) Determinants of the time course of facilitation at the granule cell to Purkinje cell synapse. *J. Neurosci.* **16,** 5661–5671
29. Llano, I., Marty, A., Armstrong, C. M., and Konnerth, A. (1991) Synaptic- and agonist-induced excitatory currents of Purkinje cells in rat cerebellar slices. *J. Physiol.* **434,** 183–213
30. Daniel, H., and Crepel, F. (2001) Control of Ca^{2+} influx by cannabinoid and metabotropic glutamate receptors in rat cerebellar cortex requires K^+ channels. *J. Physiol.* **537,** 793–800
31. Urban, J. D., Clarke, W. P., von Zastrow, M., Nichols, D. E., Kobilka, B., Weinstein, H., Javitch, J. A., Roth, B. L., Christopoulos, A., Sexton, P. M., Miller, K. J., Spedding, M., and Mailman, R. B. (2007) Functional selectivity and classical concepts of quantitative pharmacology. *J. Pharmacol. Exp. Ther.* **320,** 1–13
32. Ogawa, H., Qiu, Y., Philo, J. S., Arakawa, T., Ogata, C. M., and Misono, K. S. (2010) Reversibly bound chloride in the atrial natriuretic peptide receptor hormone-binding domain: possible allosteric regulation and a conserved structural motif for the chloride-binding site. *Protein Sci.* **19,** 544–557
33. Acher, F. C., and Bertrand, H. O. (2005) Amino acid recognition by Venus flytrap domains is encoded in an 8-residue motif. *Biopolymers* **80,** 357–366
34. Conquet, F., Bashir, Z. I., Davies, C. H., Daniel, H., Ferraguti, F., Bordi, F., Franz-Bacon, K., Reggiani, A., Matarese, V., Conde, F., Collingridge, G. L., and Crépeland, F. (1994) Motor deficit and impairment of synaptic plasticity in mice lacking mGluR1. *Nature* **372,** 237–243
35. Zucker, R. S., and Regehr, W. G. (2002) Short-term synaptic plasticity. *Annu. Rev. Physiol.* **64,** 355–405
36. Goudet, C., Magnaghi, V., Landry, M., Nagy, F., Gereau, R. W. 4th, and Pin, J. P. (2009) Metabotropic receptors for glutamate and GABA in pain. *Brain Res. Rev.* **60,** 43–56
37. Lopez, S., Turle-Lorenzo, N., Acher, F., De Leonibus, E., Mele, A., and Amalric, M. (2007) Targeting group III metabotropic glutamate receptors produces complex behavioral effects in rodent models of Parkinson's disease. *J. Neurosci.* **27,** 6701–6711
38. Hampson, D. R., Huang, X. P., Pekhletski, R., Peltekova, V., Hornby, G., Thomsen, C., and Thogersen, H. (1999) Probing the ligand-binding domain of the mGluR4 subtype of metabotropic glutamate receptor. *J. Biol. Chem.* **274,** 33488–33495
39. Rosemond, E., Peltekova, V., Naples, M., Thogersen, H., and Hampson, D. R. (2002) Molecular determinants of high affinity binding to group III metabotropic glutamate receptors. *J. Biol. Chem.* **277,** 7333–7340
40. Rosemond, E., Wang, M., Yao, Y., Storjohann, L., Stormann, T., Johnson, E. C., and Hampson, D. R. (2004) Molecular basis for the differential agonist affinities of group III metabotropic glutamate receptors. *Mol. Pharmacol.* **66,** 834–842
41. Hermit, M. B., Greenwood, J. R., Nielsen, B., Bunch, L., Jorgensen, C. G., Vestergaard, H. T., Stensbol, T. B., Sanchez, C., Krogsgaard-Larsen, P., Madsen, U., and Brauner-Osborne, H. (2004) Ibotenic acid and thioibotenic acid: a remarkable difference in activity at group III metabotropic glutamate receptors. *Eur. J. Pharmacol.* **486,** 241–250
42. Frauli, M., Hubert, N., Schann, S., Triballeau, N., Bertrand, H. O., Acher, F., Neuville, P., Pin, J. P., and Prezeau, L. (2007) Amino-pyrrolidine tricarboxylic acids give new insight into group III metabotropic glutamate receptor activation mechanism. *Mol. Pharmacol.* **71,** 704–712
43. Green, S. A., Spasoff, A. P., Coleman, R. A., Johnson, M., and Liggett, S. B. (1996) Sustained activation of a G protein-coupled receptor via "anchored" agonist binding. Molecular localization of the salmeterol exosite within the 2-adrenergic receptor. *J. Biol. Chem.* **271,** 24029–24035
44. Garavito, R. M., and Mulichak, A. M. (2003) The structure of mammalian cyclooxygenases. *Annu. Rev. Biophys. Biomol. Struct.* **32,** 183–206
45. Servant, G., Tachdjian, C., Li, X., and Karanewsky, D. S. (2011) The sweet taste of true synergy: positive allosteric modulation of the human sweet taste receptor. *Trends Pharmacol. Sci.* **32,** 631–636
46. Antony, J., Kellershohn, K., Mohr-Andra, M., Kebig, A., Prilla, S., Muth, M., Heller, E., Disingrini, T., Dallanoce, C., Bertoni, S., Schrobang, J., Trankle, C., Kostenis, E., Christopoulos, A., Holtje, H. D., Barocelli, E., De Amici, M., Holzgrabe, U., and Mohr, K. (2009) Dualsteric GPCR targeting: a novel route to binding and signaling pathway selectivity. *FASEB J.* **23,** 442–450

Received for publication September 19, 2011.
Accepted for publication December 19, 2011.